Journal of Medicinal Chemistry

Article

pubs.acs.org/jmc

Allosteric Inhibition of Human Factor XIa: Discovery of Monosulfated Benzofurans as a Class of Promising Inhibitors

Malaika D. Argade,† Akul Y. Mehta,† Aurijit Sarkar, and Umesh R. Desai*

Department of Medicinal Chemistry and Institute for Structural Biology and Drug Discovery, Virginia Commonwealth University, Richmond, Virginia 23219, United States

ABSTRACT: Factor XIa (fXIa) is being recognized as a prime target for developing safer anticoagulants. To discover synthetic, small, allosteric inhibitors of fXIa, we screened an in-house, unique library of 65 molecules displaying many distinct scaffolds and varying levels of sulfation. Of these, monosulfated benzofurans were the only group of molecules found to inhibit fXIa (~100% efficacy) and led to the identification of monosulfated trimer **24** (IC_{50} 0.82 μM) as the most potent inhibitor. Michaelis−Menten kinetics studies revealed a classic noncompetitive mechanism of action for **24**. Although monosulfated, the inhibitors did not compete with unfractionated heparin alluding to a novel site of interaction. Fluorescence quenching studies indicated that trimer **24** induces major conformational changes in the active site of fXIa. Docking studies identified a site near Lys255 on the A3 domain of fXIa as the most probable site of binding for **24**. Factor XIa devoid of the A3 domain displayed a major defect in the inhibition potency of **24** supporting the docking prediction. Our work presents the sulfated benzofuran scaffold as a promising framework to develop allosteric fXIa inhibitors that likely function through the A3 domain.

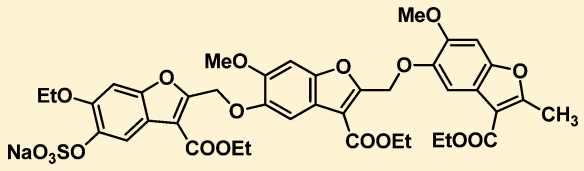

INTRODUCTION

Maintenance of hemostasis requires a delicate balance between coagulation and anticoagulation to prevent excessive bleeding while avoiding hemorrhage. Aberrant coagulation requires intervention with anticoagulants, which have primarily targeted two key proteases belonging to the common pathway of the coagulation cascade, namely, thrombin and factor Xa.[1,2] Traditionally, inhibition of thrombin and factor Xa has been considered essential to induce effective anticoagulation. Yet, knocking out these proteases also eliminates hemostatic control leading to significant bleeding.[3−7] An ideal anticoagulant would be able to parse thrombotic and hemostatic functions, and selectively modulate thrombosis. A growing paradigm in this direction is factor XIa (fXIa) as a target of anticoagulant therapy.[8]

Structurally, fXIa is a unique 160 kDa coagulation serine protease that differs from other proteases of the cascade in being a homodimer of identical subunits.[9−11] Each subunit consists of four Apple domains (labeled A1, A2, A3, and A4) composed of 90−91 amino acids each at the *N*-terminus and a trypsin-like catalytic domain (CD) at the *C*-terminus. The two subunits are held together in solution by an interchain Cys^{321}—Cys^{321} bond. The active enzyme is formed from its zymogen fXI when factor XIIa (fXIIa) cleaves the Arg^{369}—Ile^{370} bond of each subunit. The fXIa so formed then activates fIX to fIXa, which in turn sets up activation of the common pathway eventually amplifying clot formation. Interestingly, fXI can also be activated by the feedback action of thrombin, which is generated in early stages of coagulation.[12] Factor XIa can also trigger its own formation from fXI.[11] The multiple mechanisms of fXIa formation and its contribution to the amplification of the procoagulant signal suggests that regulating its catalytic activity may have a cascading effect on thrombin generation with a concomitant reduction in coagulation flux. In addition, fXIa also enhances activation of thrombin-activable fibrinolysis inhibitor, which is known to reduce the susceptibility of fibrin-rich clots to fibrinolytic agents.[13] Thus, inhibiting fXIa is expected to inhibit the generation of fibrinolysis inhibitor and help dissolve them faster through natural mechanisms, e.g., by plasmin action.

Multiple studies have highlighted fXIa as a promising target for the development of safer anticoagulants. For example, fXI-null mice were much less susceptible to arterial and venous thrombosis in comparison to wild-type mice.[14,15] More importantly, fXI-deficient mice grow healthy and do not suffer from bleeding.[15] Studies with neutralizing antibodies against fXI in rabbits also demonstrated significant defects in thrombus formation.[16] Finally, the natural deficiency of fXI, known as hemophilia C, has been reported to introduce a very benign bleeding phenotype in strong contrast to hemophilias associated with deficiencies of factors VIII and V.[17−20] Thus, targeting this upstream protease appears to be a promising strategy for developing much safer anticoagulants than those being used in the clinic today.

We have embarked on a program to discover allosteric inhibitors of human fXIa.[21,22] Allosteric regulation of fXIa has been demonstrated earlier through highly charged polyanions such as dextran sulfate, heparin, hypersulfated heparin, and sulfated pentagalloyl glucoside (SPGG).[21,23] Later work showed that synthetic molecules belonging to the monosulfated quinazolinone (QAO) scaffold were also allosteric inhibitors of

Received: February 25, 2014
Published: March 25, 2014

   dx.doi.org/10.1021/jm5002698 | *J. Med. Chem.* 2014, 57, 3559−3569

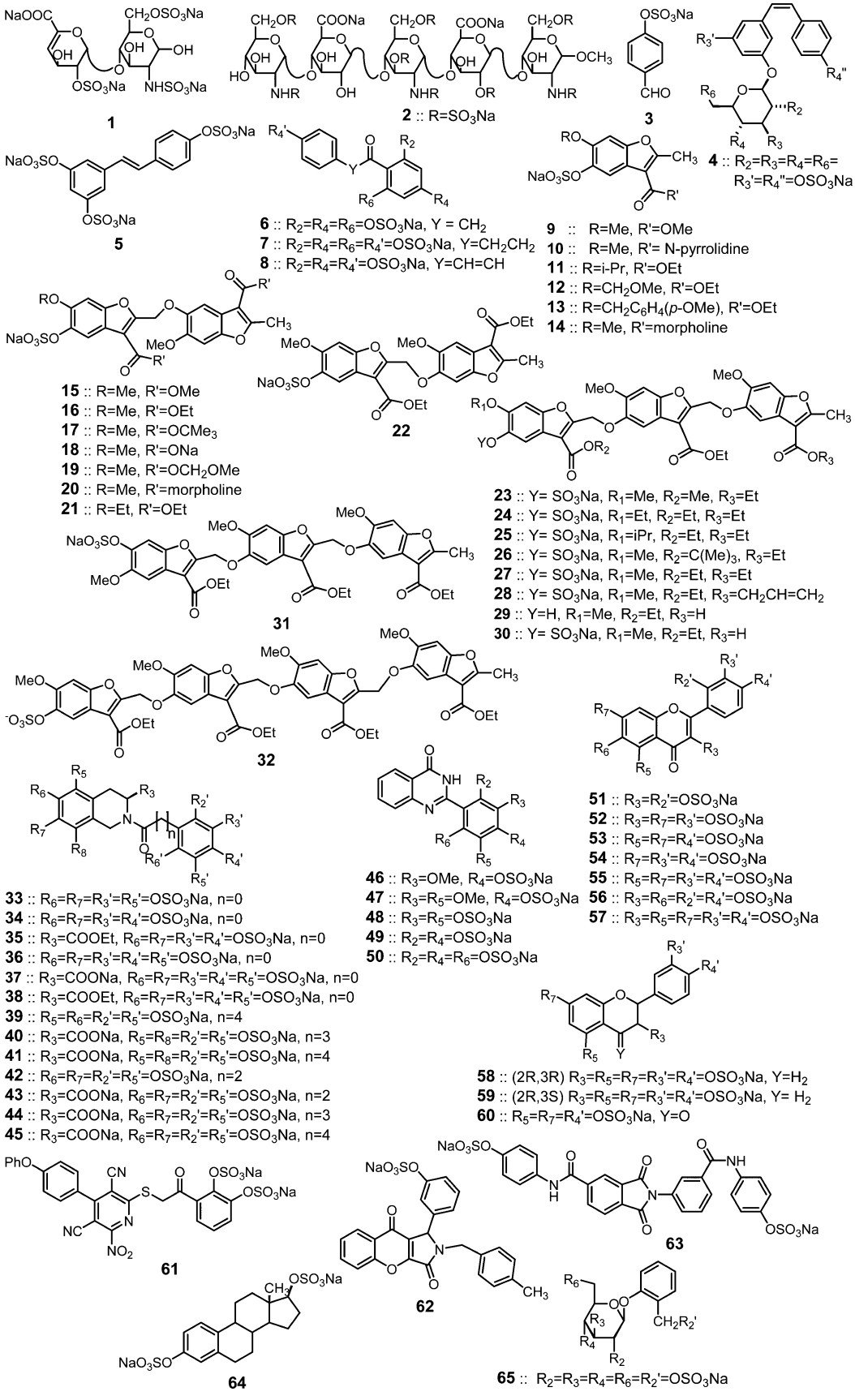

Figure 1. Structures of the sulfated small molecules constituting the library screened for factor XIa inhibition. The group of 65 molecules displayed 1 to 8 sulfate groups per molecule, more than 12 different scaffolds, and possible three-dimensional conformation from linear to globular.

dx.doi.org/10.1021/jm5002698 | J. Med. Chem. 2014, 57, 3559−3569

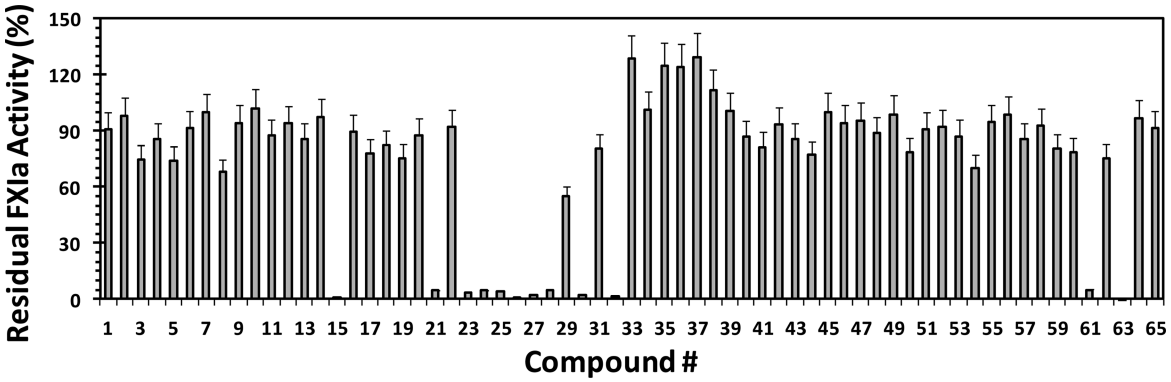

Figure 2. Medium-throughput screening of a library of 65 molecules against factor XIa in 50 mM Tris-HCl buffer, pH 7.4, at 37 °C using the chromogenic substrate hydrolysis assay. The concentration of each molecule was held constant at 300 μM. Experiments were performed at least in duplicate. The error shown represents standard deviation and was typically found to be less than 10%. The screening exercise identified not only inhibitors of factor XIa but also some activators including **33**, **35**, **36**, and **37**.

fXIa. Sulfated QAOs are the only allosteric small molecule inhibitors of fXIa reported to date.[22] Although interesting, the molecules have shown moderate potency. We reasoned that it should be possible to discover better inhibitors by screening a library of sulfated small molecules.

We present the discovery of the class of monosulfated benzofurans as promising inhibitors of human fXIa by screening an in-house library of sulfated small molecules prepared earlier. The library included 65 homogeneous molecules based on polysulfated and monosulfated scaffolds (Figure 1). These agents were synthesized in our laboratory earlier as potential modulators of coagulation, angiogenesis, and other processes.[22,24−27] A specific monosulfated benzofuran trimer was identified as the most potent molecule that reduces the catalytic activity of fXIa by binding at an allosteric site and inducing conformational changes in the catalytic triad. This work is expected to be especially useful in developing more potent allosteric inhibitors of fXIa that are based on the sulfated small molecule scaffold.

RESULTS

Rationale for Screening a Library of Sulfated Small Molecules against Factor XIa. As discussed above, our previous work led to the discovery of two classes of allosteric human fXIa inhibitors including SPGG and sulfated QAO.[21,22] Whereas SPGG was found to bind in the heparin-binding site of the enzyme, QAOs targeted a hydrophobic domain near the heparin-binding site. The fundamental reason why these groups of molecules appeared to recognize fXIa was the presence of the sulfate group(s), which invoked interaction with one or more critical basic residue(s). Interestingly, human fXIa displayed several hydrophobic domains adjacent to basic residues (see below for additional discussion on this). We reasoned that it should be possible to uncover a more potent sulfated small molecule that allosterically inhibits the enzyme by screening an in-house library (Figure 1) based on various scaffolds including sulfated flavonoids,[24,25] sulfated tetrahydroisoquinoline,[26,28,29] sulfated quinazolinone,[22] sulfated benzofurans,[30−32] and other sulfated small molecules.[26,33] Each of these sulfated small molecules had been synthesized earlier in connection with attempts to discover inhibitors or activators of other coagulation proteins (antithrombin, factor Xa, or thrombin).

As a group, the library represents at least 12 distinct scaffolds and 65 unique molecules (Figure 1) possessing one to eight sulfate groups. The library contained sulfated hydrophobic molecules possessing one to several aromatic rings, except for two saccharide-based molecules **1** and **2**. It included agents that are very small, e.g., **3**, to the considerably large, e.g., **32**, which displayed four benzofuran rings in linear sequence. A majority of the members display a projected size of ∼10−20 Å. The three-dimensional shape of these molecules have not been studied as yet; however, the orientation of different aromatic rings ensures a range of structures from primarily linear (e.g., sulfated benzofurans) to significantly globular (e.g., sulfated flavonoids). The sulfated small molecules studied here are water-soluble, but their hydrophobic character spans a large range. For example, the sulfated flavonoids **51**−**57** are considerably less hydrophobic than the sulfated benzofurans **15**−**21**, which in turn are less hydrophobic than the sulfated saccharides **1** and **2**. Finally, while the sulfated flavonoids display less conformational flexibility, the presence of linkers connecting aromatic rings in the sulfated benzofurans induces considerable flexibility. Thus, overall, our library of sulfated small molecules presents considerable configurational, conformational, and sulfate density diversity to enhance the probability of a potent hit.

Identification of Promising Inhibitors through Screening. Screening of the library against fXIa was performed using our earlier S-2366 hydrolysis assay[21,22] adopted for medium throughput conditions. Figure 2 shows the results of the screen performed at 300 μM inhibitor concentration in 50 mM Tris-HCl buffer, pH 7.4, at 37 °C. Of the 65 compounds, 12 showed a reduction in residual fXIa activity of more than 50% including **15**, **21**, **23**−**28**, **30**, **32**, **61**, and **63**. These molecules belong to the sulfated benzofuran dimer, trimer, and tetramer class of compounds, except for **61** and **63**. Yet, **61** and **63** were earlier synthesized to mimic the action of sulfated benzofurans suggesting a common structural pattern in the identified inhibitors. Interestingly, 10 monosulfated small molecules of the 25 present in the library were found to inhibit fXIa well. In contrast, only two polysulfated agents of the 40 present in the library were active. Closely related sulfated benzofurans, e.g., **22** and **31**, which are regioisomers of **16** and **27**, respectively, did not inhibit fXIa, suggesting a strong possibility of selective recognition. Of note was the observation that **29**, an unsulfated benzofuran trimer, inhibited fXIa only about 50%, while monosulfated analogues related to **29**

dx.doi.org/10.1021/jm5002698 | J. Med. Chem. 2014, 57, 3559−3569

inhibited nearly 100% suggesting a key role for the sulfate group on the benzofuran scaffold. Another interesting observation was that some sulfated small molecules enhanced fXIa catalysis by a substantial 20−30%. These included sulfated small molecules **33**, **35**, **36**, and **37** (Figure 2). These molecules are highly sulfated and belong to the tetrahydroisoquinoline class.[28,29] These factor XIa activators may be interesting from the perspective of enhancing coagulation and coagulation factor activation, especially in cases of hemophilia;[34] they are not studied further in this work.

Factor XIa Inhibition and Binding Potency of Promising Sulfated Small Molecules. Inhibitors **15**, **21**, **23**−**28**, **30**, **32**, **61**, and **63** were studied further for fXIa inhibition by measuring S-2366 hydrolysis at concentrations spanning 3 log units (Figure 3), as described earlier.[21,22] The

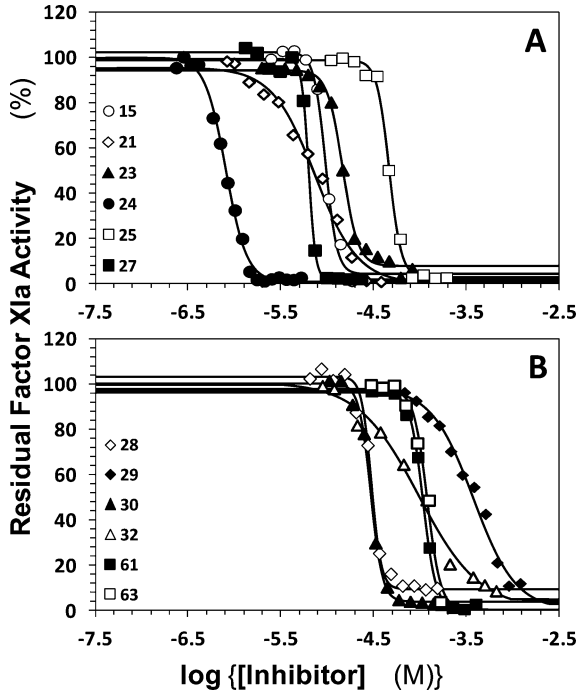

Figure 3. Direct inhibition of factor XIa by promising inhibitors discovered in the initial screen. The dose dependence of inhibition was studied using the S-2366 hydrolysis assay in 50 mM Tris-HCl buffer, pH 7.4, at 37 °C. Solid lines represent sigmoidal dose−response fits (eq 1) to obtain IC_{50}, Y_M, Y_0, and HS of inhibition. Inhibitors **21**, **24**, and **27** were identified as the most potent of the group (see Table 1).

decrease in the initial rate of fXIa activity as a function of sulfated small molecule concentration was analyzed using the logistic dose−response eq 1 to calculate inhibition parameters. Each molecule studied exhibited ∼100% efficacy (Y_M−Y_0, Table 1), while displaying a large range of potency (0.82−384 μM). The Hill slopes of the profiles ranged from 1.3 to 11.7 indicating that a majority of the inhibitors were likely to exhibit high level of cooperativity, as also observed earlier in the study of sulfated QAOs.[22] Of the group, inhibitors **24** (IC_{50} 0.82 μM), **27** (6.4 μM), **21** (7.5 μM), and **15** (9.7 μM) were found to be the most potent (Table 1). Whereas **15** and **21** are monosulfated benzofuran dimers, while **24** and **27** are trimers (Figure 1). Not many potent inhibitors of human fXIa are known, as described in the Introduction, and the discovery of a submicromolar inhibitor bodes well for further realization of a clinically relevant sulfated small molecule.

Table 1. Human Factor XIa Inhibition by Sulfated Small Molecules[a]

	IC_{50} (μM)[b]	Y_M[b]	Y_0[b]	HS[b]
15	9.7 ± 0.3[c]	102 ± 2	4 ± 4	6.9 ± 1.2
21	7.5 ± 0.6	95 ± 3	0 ± 2	1.9 ± 0.3
23	14.9 ± 0.3	94 ± 1	7 ± 1	5.2 ± 0.4
24	0.82 ± 0.02	99 ± 2	0 ± 1	3.8 ± 0.3
25	47.2 ± 0.9	99 ± 2	3 ± 2	6.6 ± 0.8
27	6.4 ± 0.1	99 ± 2	2 ± 1	11.7 ± 1.5
28	29.9 ± 0.8	103 ± 2	10 ± 2	6.4 ± 0.9
29	384 ± 38	98 ± 4	0 ± 1	1.9 ± 0.4
30	29.9 ± 0.5	100 ± 2	3 ± 2	6.9 ± 0.7
32	99 ± 13	101 ± 5	0 ± 1	1.3 ± 0.2
61	109 ± 2	96 ± 1	0 ± 1	6.2 ± 0.5
63	122 ± 3	98 ± 2	0 ± 1	6.0 ± 0.9

[a]Inhibition was measured using the chromogenic substrate hydrolysis assay as a function of inhibitor concentration in 0.05 M Tris-HCl buffer, pH 7.4, containing 0.15 M NaCl, 0.1% PEG8000, and 0.02% Tween80 at 37 °C. [b]IC_{50}, Y_M, Y_0, and HS values were obtained through nonlinear curve fitting of the dose−response profile using logistic eq 1. [c]Errors represent ±standard deviation of the mean from at least two measurements.

To further assess whether inhibition was arising due to the interaction of inhibitors with fXIa, the affinity of **21** and **24** was measured using fluorescence spectroscopy. A fluoresceinylated fXIa with labeling at the active site was used to assess the interaction in 50 mM Tris-HCl buffer, pH 7.4, at 37 °C. A decrease of 36 ± 1 and 52 ± 2% in the fluorescence emission at 522 nm was observed for both **21** and **24**, respectively, suggesting change in electrostatics around the active site due to the interaction with the two inhibitors (Figure 4A). The equilibrium dissociation constants calculated using eq 2 were found to be 4.5 ± 0.35 μM for **21** and 1.2 ± 0.3 μM for **24**. These constants are in the same range of IC_{50}, as expected, on the basis of direct inhibition.

Michaelis−Menten Kinetic Studies in the Presence of 21 and 24. Considering that blocking the active site with a fluorophore (above) did not disrupt the interaction of **21** and **24** with fXIa, we suspected an allosteric mechanism of inhibition for these interesting molecules. Typically, allosteric inhibitors display noncompetitive Michaelis−Menten kinetics, as noted for a wide range of sulfated inhibitors of coagulation enzymes.[21,22,31,32] To assess the mechanism of inhibition, studies on the rate of substrate hydrolysis were performed using a wide range of S-2366 concentrations (0.01−1.6 mM) in the presence of fixed concentrations of **21** (not shown) and **24** (Figure 4B). Analysis of the profiles using the traditional Michaelis−Menten kinetic equation showed that both inhibitors reduced the V_{MAX} in a dose-dependent manner without a significant change in the K_M (Table 2). This is characteristic of noncompetitive inhibition and illustrates that these inhibitors bind at a site away from the active site.

Induction of Conformational Changes in the Active Site of Factor XIa by 24. To further confirm the nature of the allosteric effect, we utilized collisional quenching experiments. We reasoned that if inhibitor **24** induces conformational changes in the active site, then a nonspecific, small collisional quencher, such as iodide, would reduce fluorescence emission of the active site probe at a rate different from that for the native enzyme. The phenomenon relies on direct molecular contact of sodium iodide with the fluorophore, which quenches

dx.doi.org/10.1021/jm5002698 | J. Med. Chem. 2014, 57, 3559−3569

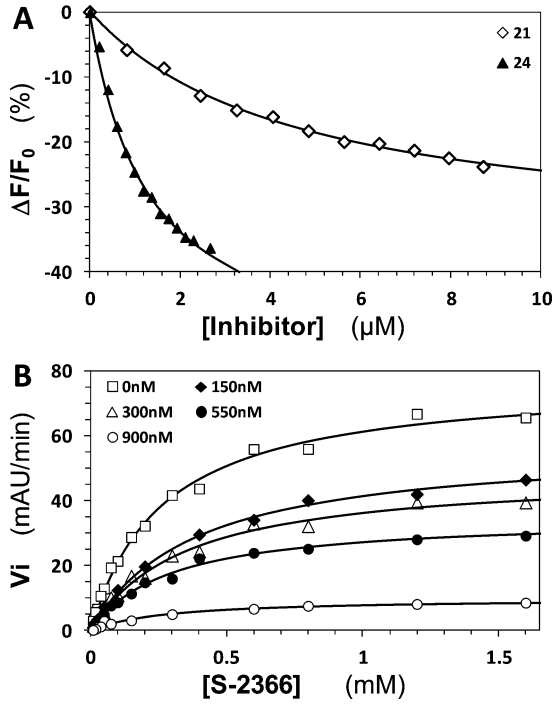

Figure 4. (A) Fluorescence-based measurement of the affinity of **21** and **24** for factor XIa in 20 mM Tris-HCl buffer, pH 7.4, at 37 °C. The decrease in fluorescence of fluorescein-labeled EGR-fXIa (λ_{EX} = 480 nm; λ_{EM} = 522 nm) upon binding of either inhibitor was fitted using quadratic binding eq 2 (solid lines) to calculate the K_D of the inhibitor–fXIa complex. (B) Michaelis–Menten kinetics of S-2366 hydrolysis in the presence of inhibitor **24**. The initial rate of substrate hydrolysis was measured in 50 mM Tris-HCl buffer, pH 7.4, at 37 °C in the presence of 0, 150, 300, 550, and 900 nM **24**. The solid lines represent nonlinear regression fits of the data by the standard Michaelis–Menten hyperbolic equation to derive the K_M and V_{MAX} of substrate hydrolysis.

Table 2. Michaelis–Menten Kinetics of Human Factor XIa Hydrolysis of S-2366 in the Presence of 21 and 24[a]

	V_{MAX} (mAU/min)	K_M (mM)
	21[b]	
0 μM	43.1 ± 0.6[c]	0.25 ± 0.01
5 μM	37.4 ± 1.4	0.23 ± 0.02
7.25 μM	30.7 ± 0.6	0.25 ± 0.01
10 μM	20.3 ± 1.2	0.31 ± 0.04
	24[d]	
0 nM	77.4 ± 1.7	0.26 ± 0.02
150 nM	57.1 ± 1.8	0.38 ± 0.03
300 nM	48.7 ± 1.7	0.35 ± 0.03
550 nM	34.9 ± 0.9	0.29 ± 0.02
900 nM	9.8 ± 0.5	0.28 ± 0.04

[a] K_M and V_{MAX} were measured by monitoring the initial rate of factor XIa hydrolysis of S-2366 from the linear increase in A_{405} in the presence of fixed concentrations of **21** and **24** in 50 mM Tris-HCl buffer, pH 7.4, at 37 °C. The data were fitted using the standard Michaelis–Menten equation to obtain K_M and V_{MAX}, as described in Experimental Procedures. [b] The concentrations of factor XIa and S-2366 were 0.365 nM and 0–1.6 mM. [c] Errors represent ±standard deviation of the mean from at least two measurements. [d] The concentrations of factor XIa and S-2366 were 0.765 nM and 0–1.6 mM.

fluorescence from the excited state.[35] Typically, reduction in the molecular accessibility of the fluorophore, arising from an altered conformation or orientation, retards iodide's quenching effect.

Figure 5A shows the iodide-induced fluorescence quenching of active-site-labeled *f*EGR-fXIa. For the enzyme alone, as the

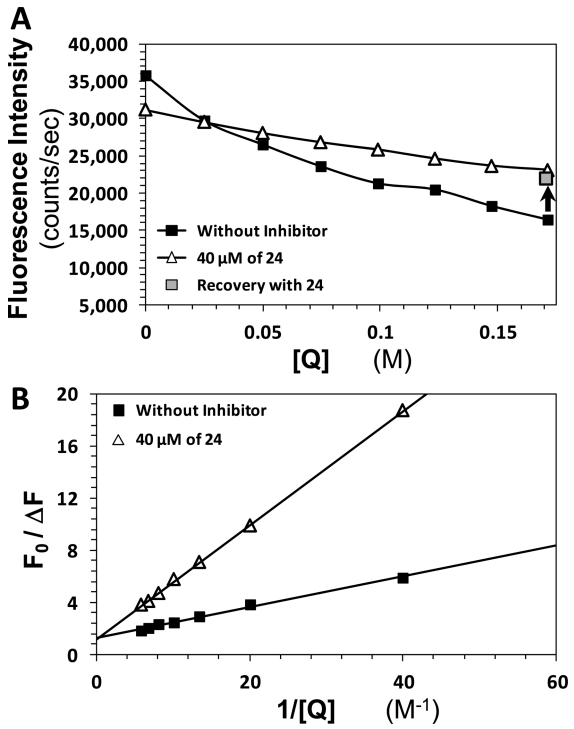

Figure 5. (A) Profile of the decrease in fluorescence intensity of active site labeled fluorescein-EGR factor XIa (λ_{EX} = 480 nm; λ_{EM} = 522 nm) as a function of the quencher concentration [Q] in the absence (Δ) and presence (■) of inhibitor **24**. The arrow shows the recovery of fluorescence upon the addition of a bolus of **24** at 0.175 M quencher, which matches the fluorescence of the titration in the presence of 40 μM **24**. (B) Stern–Volmer analysis of the quenching results presented above. Solid lines represent the linear fit to the data as predicted by the Stern–Volmer equation. The slopes of the linear fits are significantly different suggesting a change in the conformation of the active site of factor XIa upon interaction with **24**.

concentration of sodium iodide increased gradually to 0.175 M the fluorescence decreased nearly 50%, as expected. However, in the presence of saturating concentrations of **24** the rate of quenching was significantly lower (Figure 5A). Additionally, a bolus of inhibitor **24**, so as to give ~33 μM concentration in fXIa solution, quenched with 0.175 M NaI resulted in a nearly full recovery of fluorescence to levels observed for the titration in the presence of **24**. This suggested a fully reversible nature of interaction between **24** and fXIa.

Quantitative analysis of collisional quenching results can be performed using the Stern–Volmer theory.[35] For dynamic quenching at low quencher concentrations, the incremental change in fluorescence (DF) as a function of the quencher concentration ([Q]) is defined by the double reciprocal relationship (below) in which F_0 is the fluorescence intensity of the fluorophore in the absence of quencher, and K_{SV} is the Stern–Volmer constant. The Stern–Volmer plot is shown in Figure 5B. Linear regression of the data indicates that the *y*-intercept for both fXIa alone and fXIa–**24** complex is ~1, as

dx.doi.org/10.1021/jm5002698 | J. Med. Chem. 2014, 57, 3559–3569

predicted by the equation, and is indicative of the presence of only one type of fluorophore species in solution under the experimental conditions.

$$\frac{F_0}{\Delta F} = \frac{1}{K_{SV}[Q]} + 1$$

More importantly, K_{SV} decreased dramatically from 8.5 ± 0.3 for fXIa alone to 2.3 ± 0.1 for the fXIa−**24** complex. This implies that in the presence of **24** the active-site fluorophore is less accessible. Theoretically, such a change can be observed if either the ligand binds close to the fluorophore and sterically reduces the molecular accessibility of iodide or the ligand binds at an allosteric site and induces a change in the conformation of the active site, thereby altering fluorophore accessibility. Considering that the hydrodynamic volume of the quencher is small, which enables penetration into small cavities, the possibility of steric reduction of quenching effectiveness by **24** is less likely. In addition, Michaelis−Menten kinetics shows no K_M defect, which could be expected if the fluorophore and **24** bound very close to each other. Thus, Stern−Volmer analysis predicts that inhibitor **24** induces a conformational change in the active site of fXIa. This conformational change is likely to be felt by the enzyme's catalytic triad resulting in inhibition.

Do Sulfated Small Molecules Bind in the Heparin Binding Site of Factor XIa? Our previous work on allosteric inhibitors of fXIa showed them to be either ideal or partial competitors of heparin.[21−23] We suspected that inhibitors **21** and **24** may also display a similar feature considering their sulfated scaffold. Therefore, we performed competitive inhibition studies for both molecules in the presence of varying levels of unfractionated heparin (UFH). Heparin binds to FXIa in two sites: in the A3 domain (Lys252, Lys253, and Lys255) and in the catalytic domain (Lys529, Arg530, Arg532, Lys535, and Lys539). Varying affinities have been reported for this interaction from 8.6 nM to 1.5 μM.[21,22,36−39] Hence, we chose to use UFH concentrations in the range of 0 to 16 μM to assess competition rigorously, if any. Figure 6 shows fXIa inhibition by **21** and **24** in the presence of UFH. Surprisingly, no significant change in the IC_{50} of these inhibitors was observed in the presence of UFH. This indicates that **21** and **24** do not compete with UFH for binding to fXIa. Alternatively, the result indicates that the molecules probably bind to allosteric sites that do not impede simultaneous interaction with UFH.

Prediction of Site of Binding Using Molecular Docking Studies. We reasoned that molecular modeling may identify the site of binding of inhibitor **24**. Docking studies have been used earlier, especially for sulfated benzofuran oligomers binding to exosite 2 of thrombin.[31−33,40] However, docking studies with fXIa are not as straightforward considering that the crystal structure of full-length fXIa containing its four Apple domains is not available. Yet, the crystal structures of the full-length zymogen form of fXIa, i.e., fXI,[41] and the catalytic domain of fXIa are available,[42] which offer an interesting opportunity to generate a reasonable chimeric model of full-length fXIa from the two. The chimeric full-length fXIa was generated by replacing the inactive catalytic domain from the zymogen structure of fXI with that of fXIa. Interestingly, the chimera did not display any significant steric clashes, and minor clashes could be resolved by a simple energy minimization procedure. The catalytic domains of fXI and fXIa showed an overall RMSD of 0.44 Å for backbone atoms. Thus, the chimeric model appeared to be a reasonable model of full-length fXIa in solution.

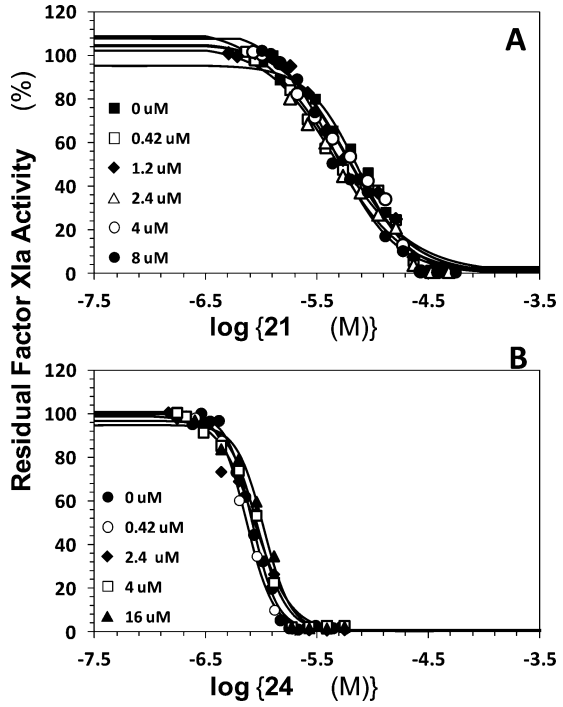

Figure 6. Absence of the competitive effect of unfractionated heparin UFH on the inhibition of factor XIa by **21** (A) and **24** (B) in 50 mM Tris-HCl buffer, pH 7.4, at 37 °C. The concentration of UFH used in the experiments was in the range of 0 to 16 μM. Solid lines represent fits using the logistic eq 1 to obtain the apparent IC_{50}, as described in Experimental Procedures.

Considering that little information was at hand on the possible site of binding, we reasoned that monosulfated benzofuran trimer **24** would bind to wild-type fXIa utilizing a dual element strategy involving (1) initial attraction of its 5-OSO_3^- group to one or more exposed Arg/Lys followed by (2) engagement of an adjacent hydrophobic patch to form a tight complex. We proposed this strategy earlier in the design of monosulfated QAOs and monosulfated benzofurans as inhibitors of fXIa and thrombin, respectively.[22,31−33] Additionally, the current inhibition results also support the possibility of dual element strategy considering that the scaffold containing only one -OSO_3^- group appeared to induce inhibition.

To assess the hypothesis of the dual element recognition more quantitatively, we studied the full-length fXIa model and identified eight sites on the protein surface displaying a relatively higher positive charge density and adjacent to a hydrophobic patch. These sites were centered around residues Lys8, Arg136, Gln153, Lys252, Lys325, Lys357, Asn566, and Arg584 (Figure 7A), which were stochastically selected as possible binding sites of inhibitor **24**. All residues within 24 Å around the identified Arg/Lys were defined as the binding site for molecular docking purposes. This operation covered practically the entire protein surface, thus ensuring exhaustive exploration for identification of possible binding site(s). Inhibitor **24** was docked at each of these eight sites using a genetic algorithm-based docking and scoring technique, as developed in the literature.[43,44] We focused primarily on consistency of docking, as evident by the RMSD between docked poses, following multiple docking runs to derive

dx.doi.org/10.1021/jm5002698 | J. Med. Chem. 2014, 57, 3559−3569

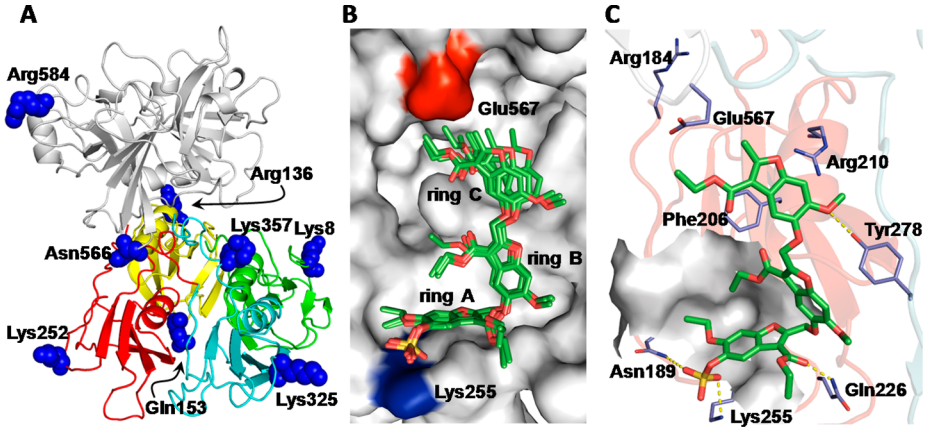

Figure 7. Genetic algorithm-based docking studies to identify a putative binding site of **24** on factor XIa. (A) Plausible sites of binding were identified by searching for hydrophobic subdomains in the vicinity of a basic (Arg/Lys) residue that could engage the sulfate group and aromatic scaffold of **24**. Eight plausible sites in the vicinity of Lys8, Arg136, Gln153, Lys252, Lys325, Lys357, Asn566, and Arg584 (shown as blue van der Waals atom spheres) were identified by generating a chimeric model from the crystal structure of the catalytic domain (PDB ID: 1ZOM) and the heavy chain of factor XI (the zymogen, PDB ID: 2F83). (B) One specific site of docking near Lys255 was identified by GOLD as the most probable binding site of **24**. GOLD predicted docking solutions within 1.6 Å RMSD suggesting highly selective recognition. Rings A, B, and C refer to the three benzofuran rings of **24**. (C) Close-up of the **24**–factor XIa docked complex showing engagement of Lys255, Asn189, Tyr278, and Gln226, each of which shows ionic or hydrogen bond interactions, and plausible π–cation interaction with Arg210 and π–π interaction with Phe206. The site is adjacent to Arg184 known to play an important role in factor IX activation by factor XIa. See text for details.

meaningful results, as suggested in earlier studies with sulfated molecules.[32,40,44]

The docking results suggested that the site around Lys252, present in the A3 domain of fXIa, was the only binding site that displayed high consistency of binding. Five out of six docked poses of **24** in this site displayed a RMSD of 1.6 Å (Figure 7B), which is much lower than the literature suggested cutoff of 2.5 Å for specific recognition.[44−46] An analysis of the atomic level interactions that appear to contribute to recognition of the site around Lys252 suggests that **24** engages Lys255, Asn189, Tyr278, and Gln226 residues. Lys255 and Asn189 are predicted to form ionic/hydrogen-bonding-type interactions with the 5-OSO_3^- group of **24**, while Gln226 and Tyr278 are predicted to hydrogen bond to benzofuran rings A and C (Figure 7C). In addition, Arg210 appears to form a π–cation interaction with benzofuran ring C, and Phe206 is located within π–π stacking distance with the same benzofuran ring. The model predicts that nearly all components of the monosulfate benzofuran trimer interact with the site around Lys252, thereby favoring specific recognition.

The predicted binding geometry of **24** on the A3 domain of fXIa explains the SAR of the benzofuran trimers quite well. The 5-OSO_3^- group present on benzofuran ring A is essential for activity because it forms strong interactions with Lys255. To quantitatively evaluate its loss, we measured the inhibition potency of **29** and found it to be 384 ± 38 μM (Figure 8A), a nearly 13-fold loss in activity from its sulfated analogue **30** (Table 1). The 6-ethoxy group of benzofuran ring A of **24** is predicted to favorably occupy a shallow hydrophobic subpocket (IC_{50} 0.82 μM). This subpocket can presumably accommodate smaller groups, e.g., the methoxy group of inhibitors **23** (IC_{50} 14.9 μM) and **27** (IC_{50} 6.4 μM) but not bulkier groups, e.g., the isopropoxy group of **25** (IC_{50} 47 μM) (see Figure 1 and Table 1). Finally, the model also explains the weaker IC_{50} of inhibitor **30** (29.9 μM) reasonably well. Inhibitor **30**, which contains a 3-carboxylate group in benzofuran ring C, appears to be 4.7-fold less potent than its 3-carboxyethyl ester analogue **27**, possibly

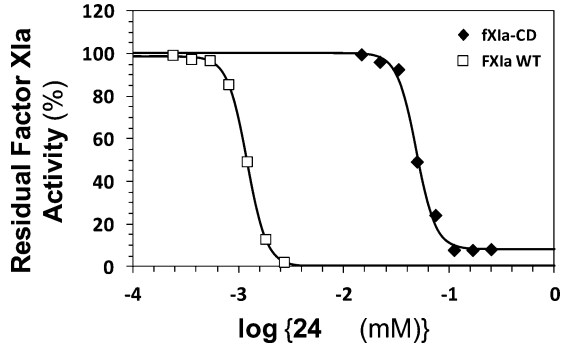

Figure 8. Loss in inhibition potency of **24** upon removal of the A3 domain containing the putative site of binding. Inhibitor **24** shows a 50-fold higher IC_{50} against the catalytic domain of factor XIa (□, fXIa-CD) in comparion to that against the wild-type fXIa (♦). The dose dependence of inhibition was studied using the S-2366 hydrolysis assay in 50 mM Tris-HCl buffer, pH 7.4, at 37 °C. Solid lines represent sigmoidal dose–response fits (eq 1).

because of the unfavorable interactions of the anionic group within the primarily hydrophobic binding pocket.

Interestingly, the predicted site of binding of **24** involves Lys255, which is known to interact with UFH.[37,38] As stated above, heparin binds at two sites on full-length fXIa. Whereas the site on the enzyme's catalytic domain is known to be allosterically coupled to the active site, the site on the A3 domain was thought of as primarily contributing to the bridging mechanism of fXIa inhibition.[10,36] This work predicts that the A3 site may also be allosterically linked to the active site. This prediction is novel and valuable for the design of advanced analogues, yet it is important to note that the computational results will require further support from site-directed mutagenesis and/or crystallography studies.

It is not clear at this time why UFH does not compete with **24** (Figure 6), although both appear to utilize Lys255. One plausible reason is that UFH binds to the A3 domain with a weaker affinity than its interaction with the catalytic domain. Comparative SPR studies have shown that full-length fXIa

dx.doi.org/10.1021/jm5002698 | J. Med. Chem. 2014, 57, 3559−3569

binds UFH with 8.6 nM affinity, which is virtually identical to that of the fXIa catalytic domain alone (11.2 nM).[36] Thus, the 16 μM UFH concentration used in competition experiments may not have saturated the A3 binding site fully resulting in a lack of competition. Another much more plausible explanation is the role of hydrophobic forces for inhibitor **24** binding to fXIa. It is possible that the highly ionic UFH utilizes a polar protein interface that avoids the hydrophobic interface utilized by inhibitor **24**. In fact, other residues of the heparin-binding site containing Lys255, i.e., Lys252 and Lys253, are located away from the site of predicted binding site of **24**. This means that although the two molecules utilize Lys255, their orientations are likely to be completely different resulting in the absence of competition.

Inhibition of the Catalytic Domain of Factor XIa. A good avenue to test the above model of the fXIa−**24** complex is site-directed mutagenesis. Unfortunately, these mutants of fXIa are not available immediately. However, we reasoned that if the A3 domain is involved in this process, then the **24** inhibition potential would be impaired by its removal. To test this, we studied the inhibition of the catalytic domain of factor XIa (fXIa-CD), which is devoid of all Apple domains, by **24** (Figure 8B). The results show that fXIa-CD was inhibited with an IC_{50} of 49 ± 2 μM suggesting a ∼40-fold loss in potency from the full-length fXIa (1.2 ± 0.2 μM). This significant loss in activity supports the modeling prediction but also suggests that our monosulfate benzofuran trimer **24** may engage the catalytic domain alone with much weaker affinity. Such dual recognition is not unusual considering that UFH also displays two binding sites.[36−39] Thus, we predict that inhibitor **24** (and possibly other monosulfated benzofurans) bind to fXIa primarily in the A3 domain near Lys255 and induce the conformational disruption of its catalytic site, resulting in inhibition.

■ DISCUSSION

This work presents the discovery of a class of monosulfated benzofurans as human fXIa inhibitors. Specifically, a monosulfated benzofuran trimer (**24**) was found to be most promising inhibitor. In comparison to our earlier studies, **24** is nearly 50-fold more potent than the best sulfated QAO designed earlier.[22] In fact, a monosulfated benzofuran dimer (**21**) also shows 10-fold improvement from earlier work, and several other analogues were moderately potent. In addition to the improvement in inhibition realized through screening, this work presents a small group of molecules that enhance the activity of factor XIa. This observation is likely to be considerably important to developing procoagulants that may have application in the field of hemophilia. Also, this is the first time a library of this size has been studied with regard to sulfated GAG mimetics. Traditionally, it has been assumed that interactions of sulfated molecules with proteins depend only on the presence of sulfate group(s). This work shows that this assumption should be questioned because several scaffolds with higher sulfate density were completely inactive. Likewise, the structural diversity represented by the library highlights the specificity of interaction arising form the monosulfated benzofurans.

Homogenous monosulfated benzofuran dimers and trimers were designed earlier as human thrombin inhibitors based on results with oligomeric sulfated low molecular weight lignins.[31,47] Interestingly, the inhibitors target a heparin-binding site on thrombin, i.e., exosite 2, whereas competition with UFH suggested that **24** and **21** do not target the equivalent exosite on the catalytic domain of fXIa. Instead, we predict that inhibitor **24** binds to a site on the A3 domain of full-length fXIa. If future structural biology studies confirm this prediction, inhibitor **24** would be the first molecule that disrupts catalytic function through A3 recognition.

Despite variance in the putative binding sites, the respective activities of these inhibitors against the two related serine proteases, thrombin and fXIa, are essentially equivalent.[31,33] This is an interesting coincidence because the binding sites are significantly different at an atomic level. Although monosulfated benzofurans may appear to be relatively nonselective between thrombin and fXIa, further structural modification of the scaffold/groups can be expected to yield selective agents. Thus, although the affinity of **24** is the best observed so far against fXIa, these agents cannot be deemed as promising clinically relevant candidates at the present time.

Yet, the monosulfated benzofurans are interesting because of their allosteric mechanism of action. Targeting an allosteric site can potentially provide two advantages: selectivity of recognition and ability to fine-tune inhibition potential.[48−50] As compared to orthosteric sites, especially of coagulation enzymes, allosteric sites are more structurally diverse, which enhances the probability of higher selectivity. In addition, allosterism relies on energetic coupling between the active site and site of inhibitor binding, which arises in the form of conformational changes that can theoretically be modulated by appropriate inhibitor design. Orthosteric or competitive inhibition, however, blocks all activity. Thus, the observation that molecule **24** is a true allosteric inhibitors bodes well for further structure-based design of molecules that may exhibit better selectivity and tunability of inhibition.

Allosterism in the **24**−fXIa interaction was deduced from fluorescence quenching experiments, which showed a significant change in conformation in or near the active site. Inhibitor **24** induced less susceptibility of the active site fluorophore to quenching by sodium iodide. This is a classic experiment used in the literature to decipher significant conformational changes.[23,35] The results suggest that monosulfated benzofurans probably bring about a physical closing of the active site so as to restrict access to species as small as iodide. The physical closing of the active site is not expected to involve changes in the α-helix/β-sheet content of the enzyme, which implies that other techniques such as CD and FTIR are less likely to report on the allosteric nature of interactions being studied here.

How is this physical closing of the active site brought about? The A3 domain has been known to be a key regulator of factor IX activation by fXIa.[51−53] It has been suggested that Arg184 within the A3 domain undergoes a dramatic movement upon activation of zymogen fXI to fXIa. More specifically, Arg184 moves from a hindered position in its cavity in fXI, where it is bound to Ser268, Asp488, and Asn566, to an exposed orientation in fXIa so as to enable its interaction with factor IX.[51,52] Our proposed binding site of **24** is in a pocket adjacent to Arg184 (Figure 7C). It is likely that inhibitor **24** restricts the movement of the catalytic domain through its interactions with the loop that hosts Arg184 and its interacting partners including Asn566. Another way to explain the same point is that inhibitor **24** possibly transforms fXIa into its zymogen-like conformation in which Arg184 movement is hindered resulting in steric restriction on access to the active site present on the catalytic domain. This results in inhibition. This allosteric effect theory is of much interest and will be the subject of further work on structure-based design of advanced molecules.

Overall, this fundamental work has realized promising monosulfated benzofuran dimers and trimers as potent inhibitors of human fXIa. Our work shows that the molecules display an allosteric mechanism of inhibition that induces conformational changes in the enzyme's active site. Molecular modeling studies have predicted a specific recognition site for inhibitor **24** (and possibly other analogs), which is a unique site that is recognized to play a major role in fXIa biochemistry. The work highlights the idea that the A3 binding domain on full-length fXIa may be targeted for the design of advanced allosteric fXIa regulators.

EXPERIMENTAL PROCEDURES

Materials. Human factor XIa (fXIa and active-site labeled fluorescein-EGR-fXIa (*f*EGR-fXIa)) was purchased from Haematologic Technologies (Essex Junction, VT). Recombinant fXIa containing only the catalytic domain (fXIa-CD) was a gift from Dr. Alireza Rezaie (St. Louis University, MO). Chromogenic substrate S-2366 (L-pyroglutamyl-L-prolyl-L-arginine-*p*-nitroaniline) was purchased from Diapharma (West Chester, OH). Stock solutions of fXIa were prepared in 0.05 M Tris-HCl buffer, pH 7.4, containing 0.15 M NaCl and 0.1% PEG8000. The buffer used in inhibition studies was 0.05 M Tris-HCl buffer, pH 7.4, containing 0.15 M NaCl, 0.1% PEG8000, and 0.02% Tween80, while that used for all other studies was devoid of 0.02% Tween80. All of the other chemicals were of biochemical grade and purchased either from Sigma-Aldrich (St. Louis, MO) or from Fisher Scientific (Pittsburgh, PA). The sulfated small molecules used in this study were prepared earlier, as described in a series of articles,[22,24−33] and were more than 95% pure. In these studies, purity was assessed by a combination of techniques including HPLC/UPLC, HR-MS, and/or elemental analysis.

Screening of a Library of Factor XIa Inhibition. A library of 65 sulfated small molecules were screened against fXIa using a chromogenic substrate hydrolysis assay adopted to 96-well microplate format (FlexStation III, Molecular Devices, Sunnyvale, CA) following previous reports on traditional screening.[21,22] Briefly, potential inhibitors (or control solvent) and fXIa were added to pH 7.4 buffer at 37 °C so as to provide final concentrations of 300 μM and 0.765 nM, respectively, incubated for 10 min, and S-2366 added to each well to give 330 μM concentration. The initial rate of S-2366 hydrolysis (<10% substrate conversion) was then measured from the increase in absorbance at 405 nm as a function of time. The residual fXIa activity (%) was calculated from the ratio of the initial rates in the presence and absence of a potential inhibitor. At least two independent experiments were performed, and the data averaged to calculate the mean and standard deviation.

Quantification of the Inhibition of Wild-Type Factor XIa or Factor XIa−Catalytic Domain. The inhibition profile of molecules displaying more than 40% relative inhibition in the initial screen was quantified using the 96-well microplate assay, which was modified from our previous reports.[21,22] Briefly, 5 μL of fXIa (wild-type or catalytic domain) was added to 85 μL of pH 7.4 buffer followed by the addition of 5 μL of inhibitor solutions, which were prepared as serial dilutions of the stock in 2/3rd (or 5/6th) decrements. The enzyme's final concentration was 0.765 nM. The mixture was then incubated for 10 min at 37 °C followed by the addition of 5 μL of S-2366 (final concentration = 330 μM) to each well, and the initial rate of increase in A_{405} was recorded to calculate the residual activity (Y, in %), which was plotted as a function of the log of inhibitor concentration ($\log[I]_0$) and fitted using eq 1 (below) to derive the concentration of the inhibitor that results in 50% inhibition of enzyme activity (IC_{50}) and the Hill slope (HS). In this equation, Y_M and Y_0 are the maximum and minimum values of the residual activity (Y), respectively.

$$Y = Y_0 + \frac{Y_M - Y_0}{1 + 10^{(\log[I]_0 - \log IC_{50})HS}} \quad (1)$$

Fluorescence Spectroscopic Studies of Sulfated Inhibitors Binding to fXIa. The fluorescence emission spectrum of fluoresceinylated fXIa (*f*EGR-fXIa) in the presence and absence of **21** and **24** was measured by exciting at 480 nm in pH 7.4 buffer at 37 °C using a QM4 spectrofluorometer (Photon Technology International, Birmingham, NJ). The excitation and emission slit widths were set at 1 mm. A semimicroquartz cuvette having a 2 mm and 10 mm path length on the excitation and emission sides, respectively, containing 250 μL total volume and inhibitors **21** and **24** at 120 μM and 8 μM, respectively, and *f*EGR-fXIa at 74 nM was used. The wavelength of maximal fluorescence emission was found to be 522 for both **21** and **24**.

The affinity of both inhibitors was measured with a similar setup by recording the fluorescence intensity at λ_{522} nm as a function of the concentration of the ligands. The relative change in fluorescence ($\Delta F/F_0$) as a function of the inhibitor concentration could be fitted using quadratic binding eq 2 to yield the dissociation constant of interaction. In this equation, ΔF_{MAX} represents the maximal change in fluorescence observed when the enzyme is saturated with the inhibitor.

$$\frac{\Delta F}{F_0} = \frac{\Delta F_{max}}{F_0}\left\{\frac{[\text{fXIa}]_0 + [I]_0 + K_D - \sqrt{([\text{fXIa}]_0 + [I]_0 + K_D)^2 - 4[\text{fXIa}]_0[I]_0}}{2[\text{fXIa}]_0}\right\} \quad (2)$$

Collisional quenching studies were performed with sodium iodide in pH 7.4 buffer at 37 °C. The quenching of active site fluorescein fluorescence of *f*EGR-fXIa (74 nM) by NaI (0−0.175 M) was measured as reported in the literature[23] in the presence (40 μM) and absence of inhibitor **24**.

Michaelis−Menten Kinetics in the Presence of Inhibitors. The initial rate of S-2366 hydrolysis by fXIa was measured, as described earlier,[21,22] in pH 7.4 buffer at 37 °C. The concentration of substrate (0.01−1.6 mM) was varied, and the concentrations of inhibitor (0−16 μM) and enzyme (0.765 nM) were held constant. The initial rate of hydrolysis was calculated from the linear increase in A_{405} at substrate concentration. The hyperbolic profile of the initial rate versus S-2366 concentration was fitted using the standard Michaelis−Menten equation to obtain the K_M and V_{MAX} values, where V_{MAX} is the maximum velocity of the enzyme reaction, and K_M is the Michaelis−Menten constant.

Competitive Inhibition Studies Using Unfractionated Heparin as a Competitor. Inhibition of fXIa by inhibitors **21** and **24** was measured in the presence of fixed concentrations of UFH (0−16 μM) in pH 7.4 buffer at 37 °C on FlexStation III (Molecular Devices, Sunnyvale, CA). Serial dilutions of **21** and **24** stocks were made in such a manner that each dilution was 5/6th of the previous. Briefly, 5 μL of fXIa (final concentration = 1.5 nM) was added to 85 μL of pH 7.4 buffer followed by the addition of 5 μL of inhibitor solutions. The mixture was then incubated for 10 min followed by the addition of 5 μL of S-2366 (345 μM). The initial rate of S-2366 hydrolysis was measured from A_{405} increase. The apparent IC_{50} was obtained using eq 1.

Molecular Modeling Studies. A model for the full-length active fXIa was generated by replacing the inactive catalytic domain of the zymogen form (PDB ID: 2f83) with the activated catalytic domain (PDB ID: 1zom) crystal structure using Pymol, version 1.5.0.4 (Schrödinger, LLC). Further modeling was performed using the protein preparation tool of Tripos Sybyl-X, version 2.1 (www.tripos.com/sybyl). Hydrogens were added to the chimeric structure and minimized keeping all heavy atoms as aggregates. Inhibitor **24** was modeled in Sybyl and docked into the structure of the chimera using GOLD[43,44] at eight probable sites of binding without any constraints.

dx.doi.org/10.1021/jm5002698 | J. Med. Chem. 2014, 57, 3559−3569

These sites were defined as 24 Å around residues Lys8, Arg136, Gln153, Lys252, Lys325, Lys357, Asn566, and Arg584 (shown in Figure 7A). For each site, a 1000 genetic algorithm run was employed in which the early termination option was disabled. Automatic cavity detection was permitted. Each docked pose was scored using GOLDSCORE, and the top two poses were retained. Triplicate docking runs were employed to ensure the docked poses were reproducible, giving us 6 docked poses per site. Average RMSD across the docked poses was ascertained using an in-house code utilizing the OEChem toolkit, version 1.7.7 (OpenEye Scientific Software, Inc., Santa Fe, NM, USA).

AUTHOR INFORMATION

Corresponding Author

*800 E. Leigh Street, Suite 212, Richmond, VA 23219, USA. Phone: 804-828-7328. Fax: 804-827-3664. E-mail: urdesai@vcu.edu.

Author Contributions

†M.D.A. and A.Y.M. contributed equally to this work.

Notes

The authors declare no competing financial interest.

ACKNOWLEDGMENTS

This work was supported by grants HL090586 and HL107152 from the National Institutes of Health. We thank Dr. Alireza R. Rezaie of St. Louis University for the recombinant factor XIa catalytic domain. This work was supported by grant S10 RR027411 a National Center For Research Resources. We also thank Openeye for providing licenses to their software.

REFERENCES

(1) Cove, C. L.; Hylek, E. M. An updated review of target-specific oral anticoagulants used in stroke prevention in atrial fibrillation, venous thromboembolic disease, and acute coronary syndromes. *J. Am. Heart Assoc.* **2013**, *2*, e000136.

(2) Henry, B. L.; Desai, U. R. Anticoagulants. In *Burger's Medicinal Chemistry, Drug Discovery and Development*, 7th ed.; Rotella, D., Abraham, D. J., Eds.; John Wiley and Sons: New York, 2010; pp 365–408.

(3) Liew, A.; Eikelboom, J. W.; O'Donnell, M.; Hart, R. G. Assessment of anticoagulation intensity and management of bleeding with old and new oral anticoagulants. *Can. J. Cardiol.* **2013**, *29*, S34–44.

(4) Simonsen, C. Z.; Steiner, T.; Tietze, A.; Damgaard, D. Dabigatran-related intracerebral hemorrhage resulting in hematoma expansion. *J. Stroke Cerebrovasc. Dis.* **2014**, *23*, e133–134.

(5) Pfeilschifter, W.; Luger, S.; Brunkhorst, R.; Lindhoff-Last, E.; Foerch, C. The gap between trial data and clinical practice - An analysis of case reports on bleeding complications occurring under dabigatran and rivaroxaban anticoagulation. *Cerebrovasc. Dis.* **2013**, *36*, 115–119.

(6) Villa, L. A.; Malone, D. C.; Ross, D. Evaluating the efficacy and safety of apixaban, a new oral anticoagulant, using Bayesian meta-analysis. *Int. J. Hematol.* **2013**, *98*, 390–397.

(7) Cossette, B.; Pelletier, M. E.; Carrier, N.; Turgeon, M.; Leclair, C.; Charron, P.; Echenberg, D.; Fayad, T.; Farand, P. Evaluation of bleeding risk in patients exposed to therapeutic unfractionated or low-molecular-weight heparin: a cohort study in the context of a quality improvement initiative. *Ann. Pharmacother.* **2010**, *44*, 994–1002.

(8) Schumacher, W. A.; Luettgen, J. M.; Quan, M. L.; Seiffert, D. A. Inhibition of factor XIa as a new approach to anticoagulation. *Arterioscler., Thromb., Vasc. Biol.* **2010**, *30*, 388–392.

(9) Wu, W.; Sinha, D.; Shikov, S.; Yip, C. K.; Walz, T.; Billings, P. C.; Lear, J. D.; Walsh, P. N. Factor XI homodimer structure is essential for normal proteolytic activation by factor XIIa, thrombin, and factor XIa. *J. Biol. Chem.* **2008**, *283*, 18655–18664.

(10) Emsley, J.; McEwan, P. A.; Gailani, D. Structure and function of factor XI. *Blood* **2010**, *115*, 2569–2577.

(11) Geng, Y.; Verhamme, I. M.; Smith, S. B.; Sun, M. F.; Matafonov, A.; Cheng, Q.; Smith, S. A.; Morrissey, J. H.; Gailani, D. The dimeric structure of factor XI and zymogen activation. *Blood* **2013**, *121*, 3962–3969.

(12) Baglia, F. A.; Walsh, P. N. Thrombin-mediated feedback activation of factor XI on the activated platelet surface is preferred over contact activation by factor XIIa or factor XIa. *J. Biol. Chem.* **2000**, *275*, 20514–20519.

(13) Von dem Borne, P. A.; Bajzar, L.; Meijers, J. C.; Nesheim, M. E.; Bouma, B. N. Thrombin-mediated activation of factor XI results in a thrombin-activatable fibrinolysis inhibitor-dependent inhibition of fibrinolysis. *J. Clin. Invest.* **1997**, *99*, 2323–2327.

(14) Renne, T.; Oschatz, C.; Seifert, S.; Muller, F.; Antovic, J.; Karlman, M.; Benz, P. M. Factor XI deficiency in animal models. *J. Thromb. Haemost.* **2009**, *7* (Suppl 1), 79–83.

(15) Gailani, D.; Lasky, N. M.; Broze, G. J., Jr. A murine model of factor XI deficiency. *Blood Coagulation Fibrinolysis* **1997**, *8*, 134–144.

(16) Yamashita, A.; Nishihira, K.; Kitazawa, T.; Yoshihashi, K.; Soeda, T.; Esaki, K.; Imamura, T.; Hattori, K.; Asada, Y. Factor XI contributes to thrombus propagation on injured neointima of the rabbit iliac artery. *J. Thromb. Haemost.* **2006**, *4*, 1496–1501.

(17) Seligsohn, U. Factor XI deficiency in humans. *J. Thromb. Haemost.* **2009**, *7* (Suppl 1), 84–87.

(18) Gomez, K.; Bolton-Maggs, P. Factor XI deficiency. *Haemophilia* **2008**, *14*, 1183–1189.

(19) Asakai, R.; Chung, D. W.; Davie, E. W.; Seligsohn, U. Factor XI deficiency in Ashkenazi jews in Israel. *N. Engl. J. Med.* **1991**, *325*, 153–158.

(20) Duga, S.; Salomon, O. Factor XI deficiency. *Semin. Thromb. Hemost.* **2009**, *35*, 416–425.

(21) Al-Horani, R. A.; Ponnusamy, P.; Mehta, A. Y.; Gailani, D.; Desai, U. R. Sulfated pentagalloylglucoside is a potent, allosteric, and selective inhibitor of factor XIa. *J. Med. Chem.* **2013**, *56*, 867–878.

(22) Karuturi, R.; Al-Horani, R. A.; Mehta, S. C.; Gailani, D.; Desai, U. R. Discovery of allosteric modulators of factor XIa by targeting hydrophobic domains adjacent to its heparin-binding site. *J. Med. Chem.* **2013**, *56*, 2415–2428.

(23) Sinha, D.; Badellino, K. O.; Marcinkiewicz, M.; Walsh, P. N. Allosteric modification of factor XIa functional activity upon binding to polyanions. *Biochemistry* **2004**, *43*, 7593–7600.

(24) Gunnarsson, G. T.; Desai, U. R. Designing small, nonsugar activators of antithrombin using hydropathic interaction analyses. *J. Med. Chem.* **2002**, *45*, 1233–1243.

(25) Gunnarsson, G. T.; Desai, U. R. Exploring new non-sugar sulfated molecules as activators of antithrombin. *Bioorg. Med. Chem. Lett.* **2003**, *13*, 679–683.

(26) Raghuraman, A.; Riaz, M.; Hindle, M.; Desai, U. R. Rapid and efficient microwave-assisted synthesis of highly sulfated organic scaffolds. *Tetrahedron Lett.* **2007**, *48*, 6754–6758.

(27) Raman, K.; Karuturi, R.; Swarup, V. P.; Desai, U. R.; Kuberan, B. Discovery of novel sulfonated small molecules that inhibit vascular tube formation. *Bioorg. Med. Chem. Lett.* **2012**, *22*, 4467–4470.

(28) Raghuraman, A.; Liang, A.; Krishnasamy, C.; Lauck, T.; Gunnarsson, G. T.; Desai, U. R. On designing non-saccharide, allosteric activators of antithrombin. *Eur. J. Med. Chem.* **2009**, *44*, 2626–2631.

(29) Al-Horani, R. A.; Liang, A.; Desai, U. R. Designing nonsaccharide, allosteric activators of antithrombin for accelerated inhibition of factor Xa. *J. Med. Chem.* **2011**, *54*, 6125–6138.

(30) Verghese, J.; Liang, A.; Sidhu, P. P.; Hindle, M.; Zhou, Q.; Desai, U. R. First steps in the direction of synthetic, allosteric, direct inhibitors of thrombin and factor Xa. *Bioorg. Med. Chem. Lett.* **2009**, *19*, 4126–4129.

(31) Sidhu, P. S.; Liang, A.; Mehta, A. Y.; Abdel Aziz, M. H.; Zhou, Q.; Desai, U. R. Rational design of potent, small, synthetic allosteric inhibitors of thrombin. *J. Med. Chem.* **2011**, *54*, 5522–5531.

(32) Sidhu, P. S.; Abdel Aziz, M. H.; Sarkar, A.; Mehta, A. Y.; Zhou, Q.; Desai, U. R. Designing allosteric regulators of thrombin. Exosite 2 features multiple subsites that can be targeted by sulfated small molecules for inducing inhibition. *J. Med. Chem.* **2013**, *56*, 5059−5070.
(33) Sidhu, P. S.; Mosier, P. D.; Zhou, Q.; Desai, U. R. On scaffold hopping: challenges in the discovery of sulfated small molecules as mimetics of glycosaminoglycans. *Bioorg. Med. Chem. Lett.* **2013**, *23*, 355−359.
(34) Whelihan, M. F.; Orfeo, T.; Gissel, M. T.; Mann, K. G. Coagulation procofactor activation by factor XIa. *J. Thromb. Hemost.* **2010**, *8*, 1532−1539.
(35) Lakowicz, J. R. Quenching of Fluorescence. In *Principles of Fluorescence Spectroscopy*, 3rd ed.; Springer: New York, 2006, pp 278−330.
(36) Yang, L.; Sun, M. F.; Gailani, D.; Rezaie, A. R. Characterization of a heparin-binding site on the catalytic domain of factor XIa: mechanism of heparin acceleration of factor XIa inhibition by the serpins antithrombin and C1-inhibitor. *Biochemistry* **2009**, *48*, 1517−1524.
(37) Zhao, M.; Abdel-Razek, T.; Sun, M. F.; Gailani, D. Characterization of a heparin binding site on the heavy chain of factor XI. *J. Biol. Chem.* **1998**, *273*, 31153−31159.
(38) Ho, D. H.; Badellino, K.; Baglia, F. A.; Walsh, P. N. A binding site for heparin in the apple 3 domain of factor XI. *J. Biol. Chem.* **1998**, *273*, 16382−16390.
(39) Badellino, K. O.; Walsh, P. N. Localization of a heparin binding site in the catalytic domain of factor XIa. *Biochemistry* **2001**, *40*, 7569−7580.
(40) Abdel Aziz, M. H.; Sidhu, P. S.; Liang, A.; Kim, J. Y.; Mosier, P. D.; Zhou, Q.; Farrell, D. H.; Desai, U. R. Designing allosteric regulators of thrombin. Monosulfated benzofuran dimers selectively interact with Arg173 of exosite 2 to induce inhibition. *J. Med. Chem.* **2012**, *55*, 6888−6897.
(41) Papagrigoriou, E.; McEwan, P. A.; Walsh, P. N.; Emsley, J. Crystal structure of the factor XI zymogen reveals a pathway for transactivation. *Nat. Struct. Mol. Biol.* **2006**, *13*, 557−558.
(42) Lin, J.; Deng, H.; Jin, L.; Pandey, P.; Quinn, J.; Cantin, S.; Rynkiewicz, M. J.; Gorga, J. C.; Bibbins, F.; Celatka, C. A.; Nagafuji, P.; Bannister, T. D.; Meyers, H. V.; Babine, R. E.; Hayward, N. J.; Weaver, D.; Benjamin, H.; Stassen, F.; Abdel-Meguid, S. S.; Strickler, J. E. Design, synthesis, and biological evaluation of peptidomimetic inhibitors of factor XIa as novel anticoagulants. *J. Med. Chem.* **2006**, *49*, 7781−7791.
(43) Jones, G.; Willett, P.; Glen, R. C.; Leach, A. R.; Taylor, R. Development and validation of a genetic algorithm for flexible docking. *J. Mol. Biol.* **1997**, *267*, 727−748.
(44) Raghuraman, A.; Mosier, P. D.; Desai, U. R. Finding a needle in a haystack. Development of a combinatorial virtual screening approach for identifying high specificity heparin/heparan sulfate sequence(s). *J. Med. Chem.* **2006**, *49*, 3553−3562.
(45) Hu, X.; Balaz, S.; Shelver, W. H. A practical approach to docking of zinc metalloproteinase inhibitors. *J. Mol. Graphics Modelling* **2004**, *22*, 293−307.
(46) Gohlke, H.; Hendlich, M.; Klebe, G. Knowledge-based scoring function to predict protein-ligand interactions. *J. Mol. Biol.* **2000**, *295*, 337−356.
(47) Henry, B. L.; Monien, B. H.; Bock, P. E.; Desai, U. R. A novel allosteric pathway of thrombin inhibition. Exosite II mediated potent inhibition of thrombin by chemo-enzymatic, sulfated dehydropolymers of 4-hydroxycinnamic acids. *J. Biol. Chem.* **2007**, *282*, 31891−31899.
(48) Szilagyi, A.; Nussinov, R.; Csermely, P. Allo-network drugs: extension of the allosteric drug concept to protein- protein interaction and signaling networks. *Curr. Top. Med. Chem.* **2013**, *13*, 64−77.
(49) Thompson, A. D.; Dugan, A.; Gestwicki, J. E.; Mapp, A. K. Fine-tuning multiprotein complexes using small molecules. *ACS Chem. Biol.* **2012**, *7*, 1311−1320.
(50) Hedstrom, L. Serine protease mechanism and specificity. *Chem. Rev.* **2002**, *102*, 4501−4524.
(51) Geng, Y.; Verhamme, I. M.; Messer, A.; Sun, M. F.; Smith, S. B.; Bajaj, S. P.; Gailani, D. A sequential mechanism for exosite-mediated factor IX activation by factor XIa. *J. Biol. Chem.* **2012**, *287*, 38200−38209.
(52) Geng, Y.; Verhamme, I. M.; Sun, M. F.; Bajaj, S. P.; Emsley, J.; Gailani, D. Analysis of the factor XI variant Arg184Gly suggests a structural basis for factor IX binding to factor XIa. *J. Thromb. Haemost.* **2013**, *11*, 1374−1384.
(53) Samuel, D.; Cheng, H.; Riley, P. W.; Canutescu, A. A.; Nagaswami, C.; Weisel, J. W.; Bu, Z.; Walsh, P. N.; Roder, H. Solution structure of the A4 domain of factor XI sheds light on the mechanism of zymogen activation. *Proc. Natl. Acad. Sci. U.S.A.* **2007**, *104*, 15693−15698.